Thermal Transitions of ϵ Crystalline Phases of Syndiotactic Polystyrene

Paola Rizzo,* Concetta D'Aniello, Anna De Girolamo Del Mauro, and Gaetano Guerra

Dipartimento di Chimica, Università degli Studi di Salerno, via Ponte Don Melillo, 84084 Fisciano (SA), Italy

Received July 24, 2007; Revised Manuscript Received October 18, 2007

ABSTRACT: Thermal transitions of the three crystalline phases (γ, δ, and ϵ) of syndiotactic polystyrene (s-PS), presenting s(2/1)2 helices, have been compared by X-ray diffraction, differential scanning calorimetry (DSC), and dynamic-mechanical analyses. These analyses have been conducted on crystalline (δ and ϵ) films, obtained by similar solvent sorption and desorption procedures, starting from a same γ-form film. The Fourier transform Infrared (FTIR) spectra of the three films have also been compared. The obtained results indicate that the recently discovered ϵ-phase, as the already known δ-phase, is transformed in γ-phase by heating above 100 °C. However, the $\epsilon \rightarrow \gamma$ transition occurs directly without the formation, for intermediate temperatures, of a helical mesomorphic phase, as instead observed for the $\delta \rightarrow \gamma$ transition. DSC studies and FTIR measurements also suggest that the crystalline packing of the ϵ-form could be rather similar to that one of the γ-form.

Introduction

Nanoporous crystalline structures can be achieved for a large variety of chemical compounds: inorganic (e.g., zeolites),[1] metal−organic[2] as well as organic.[3] These materials, often referred as inorganic, metal−organic, and organic "frameworks", are relevant for molecular storage, recognition and separation techniques.

Recently also "polymeric frameworks", i.e., semicrystalline polymeric materials presenting a nanoporous crystalline phase, have been discovered.[4,5] In particular, for syndiotactic polystyrene (s-PS), a nanoporous crystalline phase (δ-phase) presenting two identical cavities and eight styrene monomeric units per unit cell[4] has been discovered more than a decade ago. Several studies have shown that this crystalline phase is promising for applications in chemical separations and air/water purification[6] as well as in sensorics.[7]

This host δ-phase rapidly and selectively absorbs suitable guest molecules even at very low activities, producing clathrate[8] and intercalate[9] cocrystals. Particularly relevant are s-PS cocrystals with active guest molecules, which not only reduce the guest diffusivity and prevent guest self-aggregation, but also allow to control at molecular level guest location and orientation.[5,8−10] In fact, films presenting s-PS/active-guest cocrystals have been proposed as advanced materials, mainly for optical applications (e.g., as fluorescent, photoreactive, and chromophore materials).[11]

Very recently, for the same stereoregular polymer (s-PS) a new crystalline form, named ϵ, has also been discovered.[5] This new crystalline phase is also able to form cocrystals with long and high-polarity organic guest molecules. Moreover, it has been shown that, in cocrystals obtained from the ϵ-phase, the orientation of the guest molecular planes can be parallel to the polymer host chain-axes,[5] rather than perpendicular, as generally observed[8−10] for cocrystals obtained from the δ-phase.

This ϵ "polymeric framework", being able to form stable cocrystals with low-molecular-mass molecules presenting highly polarity and high hyperpolarizability, could be in principle suitable not only for optical but also for electrical applications.[5]

* Corresponding author. E-mail: prizzo@unisa.it.

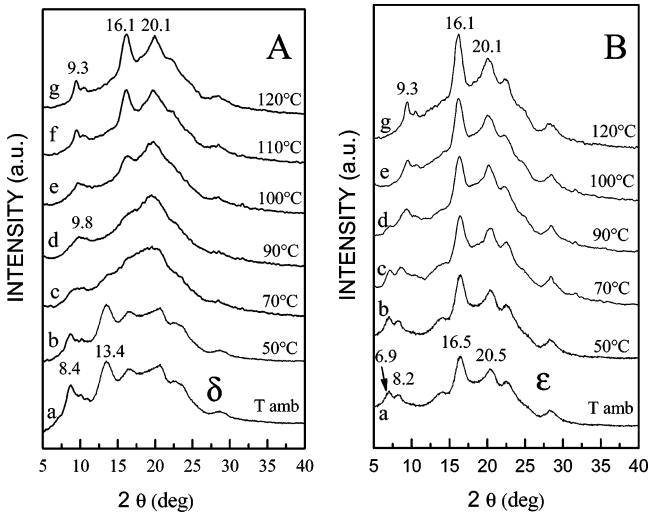

Figure 1. X-ray diffraction patterns (Cu Kα) at room temperature of essentially unoriented δ-form (A) and ϵ-form (B) films: (a) unannealed; annealed for 40 min at (b) 50, (c) 70, (d) 90, (e) 100, (f) 110, and (g) 120 °C.

In the present communication, the thermal behavior of samples presenting the recently discovered ϵ crystalline phase is shown and a comparison with the thermal behavior of the δ nanoporous phase,[12] as well as of the γ-phase,[13] is presented.

Moreover a comparison between FTIR spectra on s-PS films containing the three crystalline phases (γ, δ, and ϵ) with s(2/1)2 helical conformation, has been reported.

Experimental Section

Materials. The s-PS used in this study was manufactured by Dow Chemical Company under the trademark Questra 101. The ^{13}C nuclear magnetic resonance characterization showed that the content of syndiotactic triads was over 98%. The weight-average molar mass obtained by gel permeation chromatography (GPC) in trichlorobenzene at 135 °C was found to be $M_w = 3.2 \times 10^5$ with the polydispersity index, $M_w/M_n = 3.9$.

s-PS amorphous films, 100−120 μm thick, were obtained by extrusion of the melt with an extrusion head of 200 mm × 0.5 mm. The films are essentially amorphous and have been crystallized

10.1021/ma071640q CCC: $37.00
Published on Web 11/22/2007

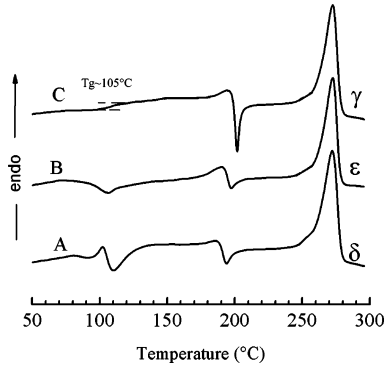

Figure 2. DSC scans for the heating rate of 10 C°/min, of the δ- (A), ϵ-, (B), and γ-form (C) films.

into the γ-form by acetone sorption at room temperature.[14] The γ-form crystallinity was then increased by annealing of the films at 140 °C for 5 h. As described in detail in ref 14, this particular procedure allows obtaining essentially unoriented γ-form films (see, e.g., Figure 9B of ref 14).

The δ-form[4a] and ϵ-form[5] films compared in this paper have been both obtained from these γ-form films. In particular, γ-form films have been treated at room temperature with carbon disulfide (for 3 days) and chloroform (for 12 h) to obtain the corresponding cocrystalline phases, which after guest removal are transformed in nanoporous δ and ϵ phases, respectively. The CS_2 guest removal has been effected by thermal treatment at 40 °C for 1 day, whereas $CHCl_3$ removal was effected by immersion in acetonitrile for 10 min. An alternative and equivalent route to prepare δ and ϵ nanoporous phases, from the corresponding cocrystals, consists of guest removal by carbon dioxide in supercritical conditions.[15]

Samples have been annealed in air, for 40 min at increasing temperatures into an ISCO oven, in the range 50−120 °C.

Methods. Wide-angle X-ray diffraction patterns with nickel filtered Cu Kα radiation were obtained, in reflection, with an automatic Bruker diffractometer.

Dynamic-mechanical properties were studied using a Triton dynamic-mechanical thermal analyzer. The spectra were recorded in the tensile mode, obtaining the modulus E', and the loss factor, tan δ, at a frequency of 1 Hz, as a function of temperature. The heating rate was 2 °C/min in the range of 0, +250 °C.

Differential scanning calorimetry (DSC) measurements were carried out with a DSC 2920 TA Instruments in a flowing nitrogen atmosphere, on 6−7 mg of films 100 μm thick at a heating rate of 10 °C/min.

Infrared spectra were obtained at a resolution of 1.0 cm^{-1} with a Vector 22 Bruker spectrometer equipped with deuterated triglycine sulfate (DTGS) detector and a Ge/KBr beam splitter. The frequency scale was internally calibrated to 0.01 cm^{-1} using a He−Ne laser. A total of 32 scans were signal averaged to reduce the noise.

The degrees of crystallinity, as evaluated by the FTIR procedure described in ref 14, are similar for all the considered s-PS films (γ, δ, and ϵ) and not far from 40%.

Results and Discussion

X-ray Diffraction. The X-ray diffraction pattern of the δ-form film (curve a in Figure 1A) is rather similar to that one of the essentially unoriented δ-form film presented in Figure 9D of ref 14 and presents the (010) peak at $d = 1.06$ nm ($2\theta_{Cu\ K\alpha} \approx 8.4°$). The X-ray diffraction pattern of the ϵ-form film (curve a in Figure 1B) is rather similar to that one of the ϵ-form powder presented in Figure 1D of ref 5b. In particular, the equatorial peaks for $d = 1.28$ nm ($2\theta_{Cu\ K\alpha} \approx 6.9°$) and $d = 1.08$ nm ($2\theta_{Cu\ K\alpha} \approx 8.2°$) typical of the ϵ-form are clearly apparent, although less intense than those for the powder sample.

Changes produced in these X-ray diffraction patterns by successive annealing procedures, for 40 min at increasing temperatures in the range 50−120 °C, are shown in Figure 1, parts A and B. The polymorphic behavior observed for the δ-form film (Figure 1A) is similar to that one described in the literature for other δ-form s-PS samples.[12] In fact, by annealing above 90 °C the nanoporous δ-phase is transformed into an "helical" mesomorphic phase which is characterized by a broader peak at $2\theta \approx 9.8°$, while by annealing above 110 °C the γ-phase, with typical (200) and (020) peaks[14b] at $2\theta_{Cu\ K\alpha} \approx$ 9.25 and 10.4° and a well-defined peak at 16.1°,[13] is obtained.

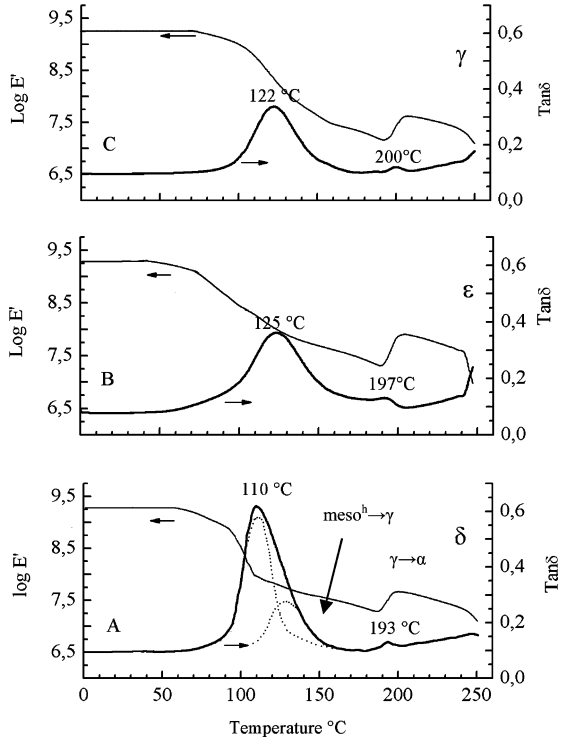

Figure 3. DMA scans for the heating rate of 2C°/min, of the δ- (A), ϵ- (B), and γ-form (C) films. For the main tan δ peak of Figure A, deconvolution curves are reported as dotted lines.

Changes of X-ray diffraction patterns of the ϵ-form film (Figure 1B) are rather different with respect to those observed for the δ-form film (Figure 1A). In fact, for the ϵ-form sample, by annealing at increasing temperatures there is a direct transformation of the ϵ-phase into a γ-phase, without transition through any mesomorphic phase. Particularly informative is, for instance, the comparison between the spectra collected after annealing at 90 °C: in fact, for the δ-form film (curve d of Figure 1A) the mesomorphic phase (with its typical broad peaks at $2\theta \approx 9.8°$ and 19.5°) is clearly present while for the ϵ-form film (curve d of Figure 1B) the γ crystalline phase has been nearly completely formed.

Differential Scanning Calorimetry. DSC scans for the heating rate of 10 °C/min, of the δ- and ϵ-form samples, whose X-ray diffraction patterns are shown by curves a of Figure 1, parts A and B, are shown in Figure 2, parts A and B, respectively. For the sake of comparison, the DSC scan of the γ-form film, from which both δ- and ϵ-form films have been prepared, is shown by curve C in Figure 2.

All the considered semicrystalline samples present a similar endothermic peak close to 270 °C corresponding to the melting of the α-phase crystallites.

All samples also present minor exothermic peaks in the temperature range 190−205 °C, corresponding to the $\gamma \rightarrow \alpha$ transition, whose position indicates that this transition occurs at higher temperature for the γ-film (200 °C) at intermediate

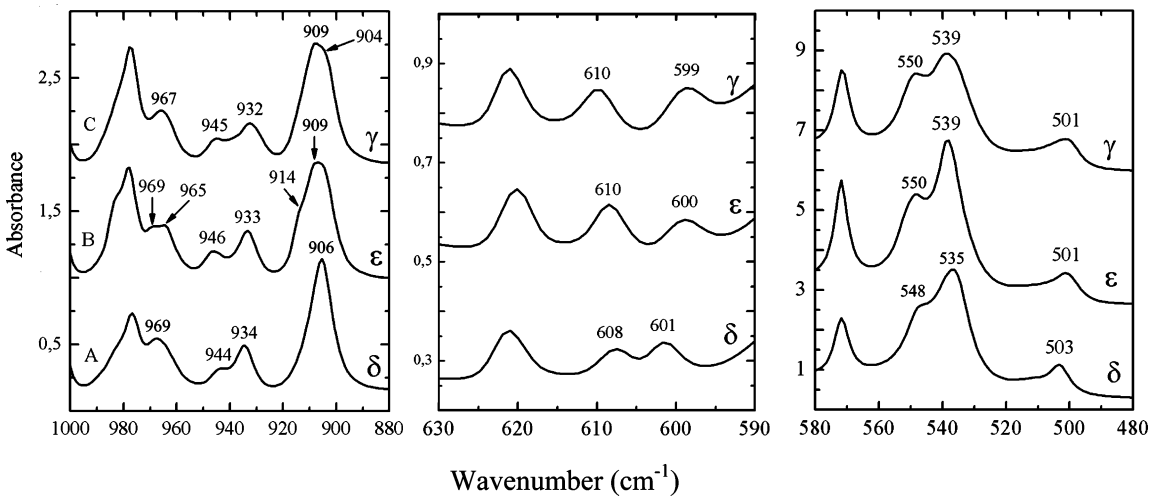

Figure 4. FTIR spectra of the δ-, ϵ-, and γ-form films of Figures 1−3, for three spectral regions presenting conformation and packing sensitive peaks. Positions of relevant peaks (in cm^{-1}) are indicated close to the curves.

temperature for the ϵ-film (197 °C) and at lower temperature for the δ-film (193 °C).

The specific heat increase typical of glass transition is clearly apparent only for the DSC scan of the γ-film and indicates $T_g \approx 105$ °C (Figure 2C). As for the DSC scans of δ- and ϵ-films, the glass transition phenomenon is hidden by their transition toward the γ-phase (Figures 2A and 2B).

As described in previous reports,[12] δ-form samples present a complex behavior in the temperature range 80−140 °C. In fact the δ-form film of Figure 2A presents a well-defined endothermic peak at 102 °C ($\Delta H \approx 2.5$ J/g) followed by an exothermic peak at 110 °C ($\Delta H \approx 5.4$ J/g). These enthalpic phenomena correspond to the above cited $\delta \rightarrow$ helical mesomorphic $\rightarrow \gamma$ thermal transitions.[12]

The DSC scan of the ϵ-form films (Figure 2B) shows only a broad and less intense exothermic phenomenon centered at 105 °C ($\Delta H \approx 2.3$ J/g). Hence, the enthalpic changes during the $\epsilon \rightarrow \gamma$ transition are much smoother than those observed for the $\delta \rightarrow \gamma$ transition. This indicates that the structural reorganization leading to the γ-phase is easier for the ϵ-phase than for the δ-phase, thus possibly suggesting some higher structural similarity.

Dynamic-Mechanical Thermal Analysis. A recent paper has shown that dynamic-mechanical thermal analysis (DMA) of s-PS samples not only is one of the most efficient techniques to determine the glass transition temperature but also is useful to study thermally induced crystal-to-crystal transitions.[16]

In this section we compare the DMA behavior of the essentially unoriented δ, ϵ and γ s-PS films of Figures 1 and 2. The DMA scans of the δ-form film (Figure 3A) is similar to that one of a clathrate film (including 8 wt % of 1,2-dichloroethane) reported in Figures 2B,C and 4 of ref 16. As already described in ref 16, this behavior is rather complex, in fact the modulus decreases abruptly in the temperature range 80−100 °C while there is a modulus recovery close to 110 °C as well a more marked recovery around 195 °C. As for the tan δ curve, beside the glass transition maximum (centered at 110 °C) and a minor maximum (centered at 193 °C), the clear asymmetry of the glass transition peak indicates the presence of a third maximum (roughly centered at 140 °C, which is more clearly apparent in the DMA scan of the uniaxially stretched film of Figure 4A of ref 16). This complex behavior has been rationalized on the basis of previous IR and X-ray diffractions data, which have shown that above T_g, δ-phase is first disordered, leading to a helical mesomorphic phase (meso^h), which in turn only at higher temperatures is reorganized into the dense γ-phase.[12] On this basis, the nature of the phase transitions has been explicitly indicated by labels close to the modulus and tan δ peaks in Figure 3A.

The DMA scan of the ϵ-form film (Figure 3B) is more simple and presents overall features similar to those of γ-form film (Figure 3C). The modulus decreases smoothly in the temperature range 80−170 °C and there is a modulus recovery above 195 °C. As for the tan δ curve, beside a nearly symmetric glass transition maximum (centered at 125 °C) there is only a minor maximum (centered at 197 °C). This more simple behavior can be rationalized on the basis of the X-ray diffractions data of Figure 1, which have shown that by annealing above T_g there is a direct transformation of the ϵ-phase into a γ-phase, without transition through any mesomorphic phase.

It is also worth adding that the temperatures corresponding to the increase of elastic modulus and the temperature of the secondary maximum of the tan δ curve, corresponding to the $\gamma \rightarrow \alpha$ transition, clearly indicate that this transition occurs at higher temperature for the γ-film (200 °C) at intermediate temperature for the ϵ-film (197 °C) and at lower temperature for the δ-film (193 °C, respectively). This confirms the information obtained from DSC exotherm peaks discussed in the previous section.

Fourier Transform Infrared Spectra. FTIR spectra of δ-, ϵ-, and γ-form films of Figures 1−3 are shown in Figure 4, for three spectral regions where conformation and packing sensitive peaks are located.

These three spectra are similar because all three crystalline phases present s(2/1)2 helices.[17] However, small differences occur in the position and intensity of some peaks, corresponding to packing sensitive vibrational modes.[18] In particular, packing sensitive peaks of the ϵ-form are more similar to those of the γ-form rather than to those of the δ-form.

For instance, for both γ- and ϵ-forms a broad absorbance band centered at 909 cm^{-1} is observed, with shoulder at 914, 904 cm^{-1}, while for the δ-form only a narrower band centered at 906 cm^{-1} is present (Figure 4A). It is worth noting that this band, mainly associated with aromatic C−H out of plane bending,[18] is particularly sensitive to the crystalline packing. In particular, this band has been widely used in the literature to afford quantitative evaluations of relative amounts of the trans-planar crystalline phases (the α and β crystalline phases presenting well resolved peaks centered at 902 and 911 cm^{-1}, respectively).[19]

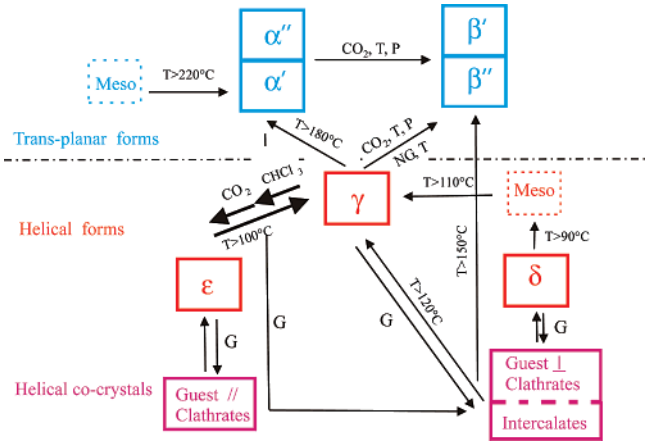

Figure 5. Schematic representation of the main interconversion conditions for the polymorphic crystalline forms of syndiotactic polystyrene. G and NG stand for molecules which are guests or nonguests of δ- and ϵ-phases. *T* and P indicate increases of temperature and pressure, respectively. Thick arrows indicate interconversion routes shown in this paper.

A similar phenomenon occurs for other peaks also involving C−H out of plane bending.[18] In particular, for both γ- and ϵ-forms, peaks at 539 and 501 cm^{-1} are observed, while for the δ-form the corresponding peaks are definitely closer, i.e., at 535 and 503 cm^{-1}(Figure 4C). Moreover, peaks at 610 and 599 cm^{-1} and at 610 and 600 cm^{-1} are observed for γ- and ϵ-films while for the δ-film closer peaks are observed at 608 and 601 cm^{-1}.

These FTIR results (as the DSC results of a previous section) suggest that the packing of the s(2/1)2 helices which occur in the ϵ-form is more similar to that one of the γ-form (presently unknown) rather than to that one (well established) of the δ-form.[4]

Schematic Presentation of Crystalline Form Interconversion Routes. In previous reports, we have presented schemes showing crystallization and interconversion routes relative to the known four crystalline forms of s-PS.[20]

In Figure 5, we have extended the scheme to the fifth crystalline forms of s-PS (ϵ), to the new kinds of s-PS cocrystals (intercalates[9] and clathrate with the orientation of the guest molecular planes parallel to the polymer host chain-axis[5]), as well as to the two (trans-planar[21] and helical[12]) mesomorphic forms.

For the sake of simplicity, we have confined the scheme to the interconversion routes without reporting crystallization conditions.

Thick arrows indicate interconversion routes shown in this paper.

Conclusions

This paper compares X-ray diffraction patterns and DMA and DSC scans as well as FTIR spectra of δ-form and ϵ-form films, obtained by similar solvent sorption procedures starting from the same γ-form film.

X-ray diffraction patterns of essentially unoriented δ-form and ϵ-form s-PS films, annealed at different temperatures, show that both crystalline forms are transformed in the γ-form. However, while for the δ-form film, as already described in the literature, this transformation involves an intermediate helical mesomorphic phase, for the ϵ-form film a direct transformation toward the γ-phase is observed.

DSC scans also point out a clearly different behavior: the $\epsilon \rightarrow \gamma$ transition produces poor enthalpic effects (only a very broad endothermic peak centered at 105 °C) while, as already well established, the $\delta \rightarrow$ mesomorphic $\rightarrow \gamma$ transition presents a well-defined endothermic peak (at 102 °C, associated with formation of the mesomorphic form) followed by an exothermic peak (at 110 °C, associated with γ-phase crystallization).

The DMA scan of the ϵ-form films is simpler than that one of δ-form films while it is similar to that one of γ-form films. Particularly relevant are the differences observed for the glass transition temperature, which is located at nearly 110 °C for the δ-form film and nearly at 125 °C for the γ- and ϵ-films. Several features of the DMA scans can be rationalized on the basis of the different routes of thermal transitions of ϵ- and δ-phases toward the γ-phase, being direct and being through a mesomorphic phase, respectively.

A careful comparison between FTIR spectra of γ, δ, and ϵ s-PS films show a definitely higher similarity between the spectra of γ- and ϵ-films, as for the location of peaks corresponding to packing sensitive modes. This FTIR analysis and the occurrence of a smoother transition toward the γ-phase suggest that the crystalline packing of the ϵ-form could be rather similar to that of the γ-form.

On the basis of results presented in this paper and in other recent papers, a more general scheme of interconversion routes between s-PS crystalline forms has been presented.

Acknowledgment. The authors thank Professor Vittorio Petraccone of University of Naples and Dr. Alexandra Albunia of University of Salerno for useful discussions. Financial support of the "Ministero dell'Istruzione, dell'Università e della Ricerca" and of "Regione Campania" (Legge 5 and Centro di Competenza per le Attività Produttive) is gratefully acknowledged.

References and Notes

(1) (a) Kuznicki, S. M.; Bell, V. A.; Nair, S.; Hillhouse, H. W.; Jacubinas, R. M.; Braunbarth, C. M.; Toby, B. H.; Tsapatsis, M. *Nature (London)* **2001**, *412*, 720−724. (b) Zecchina, A.; Bordiga, S.; Vitillo, J. G.; Ricchiardi, G.; Lamberti, C.; Spoto, G.; Bjorgen, M.; Lillerud, K. P. *J. Am. Chem. Soc.* **2005**, *127*, 6361−6366.

(2) (a) Eddaoudi, M.; Li, H.; Yaghi, O. M. *J. Am. Chem. Soc.* **2000**, *122*, 1391−1397. (b) Pan, L.; Adams, K. M.; Hernandez, H. E.; Wang, X.; Zheng, C.; Hattori, Y.; Kaneko, K. *J. Am. Chem. Soc.* **2003**, *125*, 3062−3067. (c) Kitaura, R.; Seki, K.; Akiyama, G.; Kitagawa, S. *Angew. Chem., Int. Ed.* **2003**, *42*, 428−431. (d) Millward, A. R.; Yaghi, O. M. *J. Am. Chem. Soc.* **2005**, *127*, 17998−17999.

(3) (a) Soldatov, D. V.; Moudrakovski, I. L.; Ripmeester, J. A. *Angew. Chem., Int. Ed.* **2004**, *43*, 6308−6311. (b) Blau, W. J.; Fleming, A. J. *Science* **2004**, *304*, 1457−1458. (c) Atwood, J. L.; Barbour, L. J.; Jerga, A. *Angew. Chem., Int. Ed.* **2004**, *43*, 2948−2950. (d) Sozzani, P.; Bracco, S.; Comotti, A.; Ferretti, L.; Simonutti, R. *Angew. Chem., Int. Ed.* **2005**, *44*, 1816−1820.

(4) (a) De Rosa, C.; Guerra, G.; Petraccone, V.; Pirozzi, B. *Macromolecules* **1997**, *30*, 4147−4152. (b) Milano, G.; Venditto, V.; Guerra, G.; Cavallo, L.; Ciambelli, P.; Sannino, D. *Chem. Mater.*, **2001**, *13*, 1506−1511. (c) Sivakumar, M.; Mahesh, K. P. O.; Yamamoto, Y.; Yoshimizu, H.; Tsujita, Y. *J. Polym. Sci., Part B: Polym. Phys.*, **2005**, *43*, 1873−1880. (d) Gowd, E. B.; Shibayama, N.; Tashiro, K. *Macromolecules* **2006**, *39*, 8412−8418.

(5) (a) Rizzo, P.; Daniel, C.; De Girolamo Del Mauro, A.; Guerra, G. It. Pat. N.SA2006A22. (b) Rizzo, P.; Daniel, C.; De Girolamo Del Mauro, A.; Guerra, G. *Chem. Mater.* **2007**, *19*, 3864−66.

(6) (a) Manfredi, C.; Del Nobile, M. A.; Mensitieri, G.; Guerra, G.; Rapacciuolo, M. *J. Polym. Sci., Polym. Phys. Ed.* **1997**, *35*, 133−140. (b) Guerra, G.; Manfredi, C.; Musto, P.; Tavone, S. *Macromolecules* **1998**, *31*, 1329−1334. (c) Musto, P.; Manzari, M.; Guerra, G. *Macromolecules* **1999**, *32*, 2770−2776. (d) Guerra, G.; Milano, G.; Venditto, V.; Musto, P.; De Rosa, C.; Cavallo, L. *Chem. Mater.* **2000**, *12*, 363−368. (e) Musto, P.; Mensitieri, G.; Cotugno, S.; Guerra, G.; Venditto, V. *Macromolecules* **2002**, *35*, 2296−2304. (f) Yamamoto, Y.; Kishi, M.; Amutharani, D.; Sivakumar, M.; Tsujita, Y.; Yoshimizu, H. *Polym. J.* **2003**, *35*, 465−469. (g) Saitoh, A.; Amutharani, D.; Yamamoto, Y.; Tsujita, Y.; Yoshimizu, H.; Okamoto, S. *Polym. J.* **2003**, *35*, 868−873. (h) Larobina, D.; Sanguigno, L.; Venditto, V.; Guerra, G.; Mensitieri, G. *Polymer* **2004**, *45*, 429−436. (i) Daniel,

C.; Alfano, D.; Venditto, V.; Cardea, S.; Reverchon, E.; Larobina, D.; Mensitieri, G.; Guerra, G. *Adv. Mater.* **2005**, *17*, 1515−1518. (j) Venditto, V.; De Girolamo Del Mauro, A.; Mensitieri, G.; Milano, G.; Musto, P.; Rizzo, P.; Guerra, G. *Chem. Mater.* **2006**, *18*, 2205−2210. (k) Malik, S.; Roizard, D.; Guenet, J. M. *Macromolecules* **2006**, *39*, 5957−5959.

(7) (a) Mensitieri, G.; Venditto, V.; Guerra, G. *Sens. Actuators B* **2003**, *92*, 255−261. (b) Giordano, M.; Russo, M.; Cusano, A.; Mensitieri, G.; Guerra, G. *Sens. Actuators B* **2005**, *109*, 177−184. (c) Giordano, M.; Russo, M.; Cusano, A.; Cutolo, A.; Mensitieri, G.; Nicolais, L. *Appl. Phys. Lett.* **2004**, *85*, 5349−5351. (d) Cusano, A.; Pilla, P.; Contessa, L.; Iadicicco, A.; Campopiano, S.; Cutolo, A.; Giordano, M.; Guerra, G. *Appl. Phys. Lett.* **2005**, *87*, 234105. (e) Buono, A.; Rizzo, P.; Immediata, I.; Guerra, G. *J. Am. Chem. Soc.* **2007**, *129*, 10992−10993.

(8) (a) Chatani, Y.; Inagaki, T.; Shimane, Y.; Ijitsu, T.; Yukimori, T.; Shikuma, H. *Polymer* **1993**, *34*, 1620−1624. (b) Chatani, Y.; Inagaki, T.; Shimane, Y.; Shikuma, H. *Polymer* **1993**, *34*, 4841−4845. (c) De Rosa, C.; Rizzo, P.; Ruiz de Ballesteros, O.; Petraccone, V.; Guerra, G. *Polymer* **1999**, *40*, 2103−2110. (d) Tarallo, O.; Petraccone, V. *Macromol. Chem. Phys.* **2004**, *205*, 1351−1360. (e) Tarallo, O.; Petraccone, V. *Macromol. Chem. Phys.* **2005**, *206*, 672−679.

(9) (a) Petraccone, V.; Tarallo, O.; Venditto, V.; Guerra, G. *Macromolecules* **2005**, *38*, 6965−6971. (b) Tarallo, O.; Petraccone, V.; Venditto, V.; Guerra, G. *Polymer* **2006**, *47*, 2402−2410. (c) Malik, S.; Rochas, C.; Guenet, J. M. *Macromolecules* **2006**, *39*, 1000−1007. (d) Galdi, N.; Albunia, A. R.; Oliva, L.; Guerra, G. *Macromolecules* **2006**, *39*, 9171−9176.

(10) (a) Albunia, A. R.; Di Masi, S.; Rizzo, P.; Milano, G.; Musto, P.; Guerra, G. *Macromolecules*, **2003**, *36*, 8695−8703. (b) Albunia, A. R.; Milano, G.; Venditto, V.; Guerra, G. *J. Am. Chem. Soc.* **2005**, *127*, 13114−13115.

(11) (a) Venditto, V.; Milano, G.; De Girolamo Del Mauro, A.; Guerra, G.; Mochizuki, J.; Itagaki, H. *Macromolecules* **2005**, *38*, 3696−3702. (b) Stegmaier, P.; De Girolamo Del Mauro, A.; Venditto, V.; Guerra, G. *Adv. Mater.* **2005**, *17*, 1166−1168. (c) Uda, Y.; Kaneko, F.; Tanigaki, N.; Kawaguchi, T. *Adv. Mater.* **2005**, *17*, 1846−1850. (d) Kaneko, F.; Uda, Y.; Kajiwara, A.; Tanigaki, N. *Makrom. Chem. Rapid. Commun.* **2006**, *27*, 1643−1647. (e) D'Aniello, C.; Musto, P.; Venditto, V.; Guerra, G. *J. Mater. Chem.* **2007**, *17*, 531−535. (f) Daniel, C.; Galdi, N.; Montefusco, T.; Guerra, G. *Chem. Mater.* **2007**, *19*, 3302−3308.

(12) (a) Manfredi, C.; De Rosa, C.; Guerra, G.; Rapacciuolo, M.; Auriemma, F.; Corradini, P. *Macromol. Chem. Phys.*, **1995**, *196*, 2795−2808. (b) Manfredi, C.; Guerra, G.; De Rosa, C.; Busico, V.; Corradini, P. *Macromolecules* **1995**, *28*, 6508−6515. (c) Gowd, E. B.; Shibayama, N.; Tashiro, K. *Macromolecules* **2006**, *39*, 8412−8418.

(13) (a) Immirzi, A.; De Candia, F.; Iannelli, P.; Vittoria, V.; Zambelli, A. *Makrom. Chem. Rapid. Commun.* **1988**, *9*, 761−764. (b) Guerra, G.; Vitagliano, V. M.; De Rosa, C.; Petraccone, V.; Corradini, P. *Macromolecules* **1990**, *23*, 1539−1544. (c) Rizzo, P.; Lamberti, M.; Albunia, A. R.; Ruiz de Ballesteros, O.; Guerra, G. *Macromolecules* **2002**, *35*, 5854−5860. (d) Tamai, Y.; Fukuda, M. *Macromol. Rapid Commun.* **2002**, *23*, 891−895. (e) Rizzo, P.; Albunia, A. R.; Guerra, G. *Polymer* **2005**, *46*, 9549−9554. (f) Guerra, G.; De Rosa, C.; Petraccone, V. *Polym. Networks Blends* **1992**, *2*, 1145−1151.

(14) Albunia, A. R.; Musto, P.; Guerra, G. *Polymer* **2006**, *47*, 234−242.

(15) (a) Reverchon, E.; Guerra, G.; Venditto, V. *J. Appl. Polym. Sci.* **1999**, *74*, 2077−2082. (b) Ma, W.; Yu, J.; He, J. *Macromolecules* **2005**, *38*, 4755−4760.

(16) D'Aniello, C.; Rizzo, P.; Guerra, G. *Polymer* **2005**, *46*, 11435−11441.

(17) (a) Reynolds, N. M.; Savage, J. D.; Hsu, S. L. *Macromolecules* **1989**, *22*, 2867−2869. (b) Kobayashi, M.; Nakaoki, T.; Ishihara, N. *Macromolecules* **1990**, *23*, 78−83. (c) Guerra, G.; Musto, P.; Karasz, F. E.; MacKnight, W. J. *Makromol. Chem.* **1990**, *191*, 2111−2119. (d) Tashiro, K.; Useno, Y.; Yoshioka, A.; Kobayashi, M. *Macromolecules* **2001**, *34*, 310−315. (e) Yoshioka, A.; Tashiro, K. *Macromolecules* **2003**, *36*, 3001−3003.

(18) (a) Reynolds, N. M.; Hsu, S. L. *Macromolecules* **1990**, *23*, 3463−3472. (b) Rastogi, S.; Gupta, V. D. J. *Macromol. Sci.* **1994**, *B33*, 129−141. (c) Torres, F. J.; Civalleri, B.; Pisani, C.; Musto, P.; Albunia, A. R.; Guerra, G. *J. Phys. Chem., B* **2007**, *111*, 6327−6335. (d) Albunia, A. R.; Rizzo, P.; Guerra, G.; Torres, F. J.; Civalleri, B.; Zichovich-Wilson, C. M. *Macromolecules* **2007**, *40*, 3895−3897.

(19) (a) Musto, P.; Tavone, S.; Guerra, G.; De Rosa, C. *J. Polym. Sci., Polym. Phys.* **1997**, *35*, 1055−1066. (b) Ho, R.-M.; Lin, C.-P.; Hseih, P.-Y.; Chung, T.-M.; Tsai, H.-Y. *Macromolecules* **2001**, *34*, 6727−6736. (c) Sun, Y. S.; Woo, E. M.; Wu, M. C.; Ho, R.-M. *Macromolecules* **2003**, *36*, 8415−8425.

(20) (a) Guerra, G.; De Rosa, C.; Petraccone, V. *Polym. Networks Blends* **1992**, *2*, 1145−1151. (b) Rizzo, P.; Albunia, A. R.; Guerra, G. *Polymer* **2005**, *46*, 9549−9554.

(21) (a) De Candia, F.; Filho, A. R.; Vittoria, V. *Makromol. Chem. Rapid Commun.* **1991**, *12*, 295−299. (b) Petraccone, V.; Auriemma, F.; Dal Poggetto, F.; De Rosa, C.; Guerra, G.; Corradini, P. *Makromol. Chem.* **1993**, *194*, 1335−45. (c) Auriemma, F.; Petraccone, V.; Dal Poggetto, F.; De Rosa, C.; Guerra, G.; Manfredi, C.; Corradini, P. *Macromolecules* **1993**, *26*, 3772−3777.

MA071640Q